An iterative particle filter approach for coupled hydro-geophysical inversion of a controlled infiltration experiment.

Published version:

DOI:10.1016/j.jcp.2014.11.035

(Article begins on next page)

Elsevier Editorial System(tm) for Journal Of Computational Physics
Manuscript Draft

Manuscript Number: JCOMP-D-14-00215R1

Title: An iterative particle filter approach for coupled hydro-geophysical inversion of a controlled infiltration experiment

Article Type: Regular Article

Keywords: Particle filter; Data Assimilation; Coupled Hydro-Geophysical Inversion; Electrical Resistivity Tomography

Corresponding Author: Mr. Gabriele Manoli,

Corresponding Author's Institution: University of Padova

First Author: Gabriele Manoli

Order of Authors: Gabriele Manoli; Matteo Rossi; Damiano Pasetto; Rita Deiana; Stefano Ferraris; Giorgio Cassiani; Mario Putti

Abstract: The modeling of unsaturated groundwater flow is affected by a high degree of uncertainty related to both measurement and model errors. Geophysical methods such as Electrical Resistivity Tomography (ERT) can provide useful indirect information on the hydrological processes occurring in the vadose zone. In this paper, we propose and test an iterataed particle filter method to solve the coupled hydrogeophysical inverse problem. We focus on an infiltration test monitored by time-lapse ERT and modeled using Richards equation. The goal is to identify hydrological model parameters from ERT electrical potential measurements. Traditional uncoupled inversion relies on the solution of two sequential inverse problems, the first one applied to the ERT measurements, the second one to Richards equation. This approach does not ensure an accurate quantitative description of the physical state, typically violating mass balance. To avoid one of these two inversions and incorporate in the process more physical simulation constraints, we cast the problem within the framework of a SIR (Sequential Importance Resampling) data assimilation approach that uses a Richards equation solver to model the hydrological dynamics and a forward ERT simulator combined with Archie'slaw to serve as measurement model. ERT observations are then used to update the state of the system as well as to estimate the model parameters and their posterior distribution. The limitations of the traditional sequentialBayesian approach are investigated and an innovative iterative approach is proposed to estimate the model parameters with high accuracy. The numerical properties of the developed algorithm are verified on both homogeneous and heterogeneous synthetic test cases based on a real-world field experiment.

Reply to Editor

NICHOLAS SCHOOL OF THE ENVIRONMENT
DUKE UNIVERSITY

DIVISION OF EARTH & OCEAN SCIENCES

November 18, 2014

Dear Editor,

thank you for reconsidering the manuscript *"An iterative particle filter approach for coupled hydro-geophysical inversion of a controlled infiltration experiment"* by G. Manoli, M. Rossi, D. Pasetto, R. Deiana, S. Ferraris, G. Cassiani, and M. Putti (JCOMP-D-13-00723) for publication after minor revisions.

We have addressed all the reviewer's minor comments and, in the attached documents, we report the revised version of the paper together with a summary of the revisions made.

Thank you for your time and consideration,

Gabriele Manoli

Duke University, Box 90227, Durham, NC, 27708-0227, USA • t: 919.684.5847 • f: 919.684.5833
www.nicholas.duke.edu/eos

Revision notes

"An iterative particle filter approach for coupled hydro-geophysical inversion of a controlled infiltration experiment"

(JCOMP-D-14-00215)

Reviewer #2:

The manuscript presents an iterative Bayesian approach to data assimilation in the context of hydro-geophysical inversion. I did not review the first version of this manuscript; based on the first round of reviews and the authors' reply I feel the revised version (the current submission) is a significant improvement that warrants the manuscript's eventual publication in JCP. The following are a few (relatively minor) comments that should be addressed before the manuscript becomes publishable.

1. The introduction misses a discussion of the state-of-the-art in "hydro-geophysical inversion of...infiltration experiment[s]". In the absence of such a discussion, it is hard to judge the novelty of the current contribution to that particular application area. A cursory Google search with these keywords reveals a number of papers, e.g., Tartakovsky and others, Hydro-geophysical approach for identification of layered structures of the vadose zone from electrical resistivity data, Vadose Zone Journal, 2008.

REPLY: <u>We agree with the reviewer’s comment and we have added a discussion on state-of-the-art applications of hydro-geophysical inversion for the characterization of vadose zone processes (p. 3 lines 17-20):</u>

> *“ERT has been widely used to monitor vadose zone processes (e.g., Daily et al. 1992, LaBrecque et al. 2004, Tartakovsky et al. 2008) but it is well known that the inversion procedure can produce mass balance errors (Singha and Gorelick, 2005) especially when surface ERT is used to monitor water infiltration into soil (Michot et al. 2003, Cassiani et al. 2012, Travelletti et al. 2012) due to a rapid decrease of ERT resolution with depth.”*

2. It would be helpful to provide a motivation for the computational example presented in Figure 6(a). What physical setting does this example represent? Would it not be more natural to consider a layered soil?

REPLY: <u>The reviewer is right, the choice of the physical setting presented in Fig. 6a has been clarified. Just to add to the discussion with the reviewer, we would like to point out that a layered soil with vertical-only infiltration would note test completely the ability of the method to identify spatially heterogeneous patterns. In some sense, the proposed test case actually contains the layered case, but adds also a horizontal component to the front movement. We have added the following sentence (p. 27 lines 424-427):</u>

> *“The physical setting in Fig. 6(a) is not intended to represent typical field conditions but aims to provide a simple setup generating both vertical and lateral infiltration patterns to test the proposed approach in a truly multidimensional heterogeneous setting.”*

An iterative particle filter approach for coupled hydro-geophysical inversion of a controlled infiltration experiment

Gabriele Manoli[a,b], Matteo Rossi[c], Damiano Pasetto[a], Rita Deiana[d], Stefano Ferraris[e], Giorgio Cassiani[c], Mario Putti[a]

[a] *Department of Mathematics, University of Padova, Via Trieste 63, 35121 Padova, Italy*
[b] *Nicholas School of the Environment, Duke University, Durham, North Carolina 27708, USA.*
[c] *Department of Geosciences, University of Padova, Via Gradenigo 6, 35131 Padova, Italy*
[d] *Dipartimento dei Beni Culturali, University of Padova, Piazza Capitaniato 7, 35139 Padova, Italy*
[e] *Interuniversity Department of Regional and Urban Studies and Planning, Politecnico and University of Torino, Viale Mattioli 39, 10125 Torino, Italy*

Abstract

The modeling of unsaturated groundwater flow is affected by a high degree of uncertainty related to both measurement and model errors. Geophysical methods such as Electrical Resistivity Tomography (ERT) can provide useful indirect information on the hydrological processes occurring in the vadose zone. In this paper, we propose and test an iterataed particle filter method to solve the coupled hydrogeophysical inverse problem. We focus on an infiltration test monitored by time-lapse ERT and modeled using Richards equation. The goal is to identify hydrological model parameters from ERT electrical potential measurements. Traditional uncoupled inversion relies on the solution of two sequential inverse problems, the first one applied to the

Email address: `manoli@dmsa.unipd.it` (Gabriele Manoli)

ERT measurements, the second one to Richards equation. This approach does not ensure an accurate quantitative description of the physical state, typically violating mass balance. To avoid one of these two inversions and incorporate in the process more physical simulation constraints, we cast the problem within the framework of a SIR (Sequential Importance Resampling) data assimilation approach that uses a Richards equation solver to model the hydrological dynamics and a forward ERT simulator combined with Archie's law to serve as measurement model. ERT observations are then used to update the state of the system as well as to estimate the model parameters and their posterior distribution. The limitations of the traditional sequential Bayesian approach are investigated and an innovative iterative approach is proposed to estimate the model parameters with high accuracy. The numerical properties of the developed algorithm are verified on both homogeneous and heterogeneous synthetic test cases based on a real-world field experiment.
Keywords: Particle filter, Data Assimilation, Coupled Hydro-Geophysical Inversion, Electrical Resistivity Tomography

1. Introduction

Electrical Resistivity Tomography (ERT) is a practical, cost-effective, indirect tool for collecting soil and moisture content data in subsurface environments [1–5]. When applied to the simulation of the dynamics of the vadose zone, ERT relies on the inversion of the direct current (DC) flow equation providing an image of the electrical resistivity [4], with the soil moisture pattern reconstructed from petrophysical relations, such as, e.g., Archie's Law [6]. A second inverse problem is finally used to estimate hydrological model parameters. It is well known that inverse modeling of a parabolic diffusion equation is generally an ill-posed problem and regularization techniques are often employed to achieve well-posedness [2, 7–9]. Traditional geophysical inversion is at the same time an over- and under- constrained problem, in the sense that the problem character can change in space, and benefits from the use of prior information embedded in the regularization procedure [10]. However, imposing smoothness via regularization may introduce inaccuracies or even unphysical constraints into the estimates of the hydrological properties [11]. ERT has been widely used to monitor vadose zone processes [e.g. 1, 12, 13] but it is well known that the inversion procedure can produce mass balance errors [14] especially when surface ERT is used to monitor water infiltration into soil [15, 5, 16] due a rapid decrease of ERT resolution with depth. To cope with this limitation coupled hydro-geophysical approaches seem highly promising [17]. By these procedures, the spatial distribution and the temporal dynamics of the geophysical properties are enforced by a physically based hydrologic model combined with petrophysical relations, and explicit assumptions for spatial and temporal regularization are no longer needed.

Even though the coupled approach avoids an independent geophysical inversion, estimation of the hydrologic properties (e.g. soil hydraulic parameters) is still a highly non-linear, mixed-determined inversion problem. For these reasons, although parameter estimation can be made theoretically well-posed, the physical interpretation of the estimated parameters is still not well understood [18]. The presence of structural model errors (model approximations, uncertain initial conditions, etc.), as well as measurement uncertainties, suggests that a deterministic search for the best parameters is not likely to converge to a single set of "true" values. A stochastic approach based on ensemble forecasting seems therefore the most appropriate solution procedure [18, 19].

Sequential Data Assimilation (S-DA) methods (typically called filters) have been successfully applied to improve model predictions by incorporating real system observations onto the dynamical model and have been already employed to correct the hydrological states of groundwater infiltration models [20]. Their ability to include structural and parametric error distributions make them particularly attractive for application to the problem of dynamic parameter estimation [18]. Because of the high nonlinearity of porous media infiltration models, the typical filtering method used in hydrological applications is the Ensemble Kalman filter (EnKF) [21]. Notwithstanding the linear optimality properties of the Kalman Gain [22], the main limitation of EnKF is that it is based on the Gaussian approximation of the filtering probability distribution, possibly leading to inaccurate results or even divergence of the posterior pdfs in presence of a strongly nonlinear relation between observations and state variables [23–25]. To cope with arbitrary non-Gaussian prior distributions, the family of particle filters is a highly attractive alternative, as it is directly based on the Bayesian filtering rule [26, 27]. Particle filters have been recently introduced into hydrology [28–31, 25] and used also for estimation of hydrological model parameters [32–34]. All these latter studies focus on the assimilation of direct hydrological information (e.g. discharge [25] or soil moisture data [35–37]). A coupled hydro-geophysical parameter estimation procedure by S-DA has been presented by [38], but its ability to provide accurate estimates of unknown model parameters remains to be proven, as shown by the consistent underestimation of saturated hydraulic conductivity in the results of [38]. As a matter of fact, the structural uncertainties of both the hydrologic evolution and geophysical observation models strongly affect the estimated parameters. Sequential filters correct both model parameters and state variables at each assimilation time, yielding identified parameter values that vary in time [18]. Compared to smoothers or other more sofisticated inversion methods (e.g., Markov Chain Monte Carlo methods [39, 40]) the filtering approach is computationally more efficient when dealing with a detailed and spatially resolved simulation model such as the coupled Richards equation-ERT solver here employed.

In this paper we propose an iterative procedure to overcome the problem of the sensitivity to the initial guess and provide accurate identification of unknown model parameters from indirect state information. The method is grounded on a Sequential Importance Resampling (SIR) particle filter, already tested in similar hydrological applications [25, 38], whereby an ERT forward simulation model is embedded into the observation equation and both parameter and state distributions are updated at each assimilation step. Iteration is introduced by sequentially repeating until convergence the same simulation period, using as initial guess the state values and parameter pdfs evaluated from the results of the previous iteraton. Compared to more sofisticated statistical updates, the use of iterations allows the inclusion of a less accurate but computationally more efficient inversion scheme able to cope with large dimensional problems.

We validate the methodology on synthetic test cases and apply the methods to a field experiment comparing the results of our procedure with traditional uncoupled inversion of ERT data. We focus on both homogeneous and heterogeneous systems with parameters distributed by zones. The proposed procedure displays convergence of the posterior distribution towards the correct value of the hydraulic conductivity in both the homogenous and heterogeneous scenarios independently from the initial guess. The numerical results obtained from the synthetic test cases show that the iterative approach yields faster convergence with respect to standard DA methods, using consistently smaller ensemble sizes and a drastic reduction of the number of forward model runs, in particular for the heterogeneous test case. The results obtained in the application to the real world problem are consistent with the desired physical constraints at relatively low computational costs, thus improving significantly on existing coupled flow-ERT procedures.

2. Parameter estimation by sequential data assimilation

The state space model describing the S-DA problem can be written as:

$$x_t = \mathcal{F}(x_{t-1}, \lambda, w_t), \quad (1)$$

$$y_t = \mathcal{H}(x_t, \lambda, v_t), \quad (2)$$

where x_t is the state vector at assimilation time t, $\mathcal{F}$ is the evolution operator, λ is the time-independent parameter vector, w_t is the stochastic model error, y_t is the observation vector, $\mathcal{H}$ is the observation model, and v_t is the stochastic error term in the observations. Model uncertainty is connected, e.g., to structural model errors, parameter errors, initial solution errors, etc. Casted in a stochastic framework, the objective of S-DA is to estimate the posterior probability density function (pdf) of the state vector at time t conditioned to the observations y_t^{obs} that become available at time t. Because of model nonlinearity, Monte Carlo-based approaches are used to discretize the state and observation pdfs in equations (1) and (2). To relax the Gaussian hypothesis inherent to Kalman-filter based algorithms we estimate the state and parameter pdfs employing a SIR (Sequential Importance Resampling) particle filter, which has been successfully tested in hydrological applications [25] in standard S-DA mode.

2.1. Sequential Importance Resampling for parameter estimation

Let the state vector x_t be characterized by a probability density function denoted by $p(x_t)$ and let $p(\lambda)$ be the prior distribution of the parameters λ. The sequence of random variables $\{x_0, x_1, \dots\}$ defines a Markov chain where (1) and $p(w_t)$ uniquely identify the transition probability density function $p(x_t|x_{t-1}, \lambda)$. The variance associated to $p(x_t)$ typically increases with time during the numerical simulation, leading to highly uncertain forecasts. Our goal is to obtain the posterior distribution of the parameters λ and of the state variables x_t, conditioned to the field observations $y_{1:t}^{obs}$, i.e., the filtering pdf $p(x_t, \lambda|y_{1:t}^{obs})$. Sequential data assimilation allows to compute a posterior distribution as soon as a field observation y_t^{obs} becomes available. For this reason in the following we will assume that the parameters are time dependent, λ_t, in the sense that they may change when their posterior distribution changes.

The S-DA technique consists of two basic steps that are repeated sequentially. In the forecast step the state pdf is propagated in time to obtain the forecast pdf, $p(x_t, \lambda_t|y_{1:t-1}^{obs})$. This is expressed by the Chapman-Kolmogorov equation as:

$$p\left(x_t, \lambda_t | y^{obs}_{1:t-1}\right) = \int p\left(x_t, \lambda_t | x_{t-1}, \lambda_{t-1}\right)\ p\left(x_{t-1}, \lambda_{t-1} | y^{obs}_{1:t-1}\right) dx_{t-1} d\lambda_{t-1}. \quad (3)$$

Note that in this step we have the effective propagation from time $t-1$ to time t of the system state by formal application of (1) using constant values of the parameters. The second step is called analysis or update and consists in correcting the forecast pdf using the new field observation y^{obs}_t. Bayes' theorem allows the factorization of the filtering pdf as:

$$p\left(x_t, \lambda_t | y^{obs}_{1:t}\right) = Cp\left(y^{obs}_t | x_t, \lambda_t\right) p\left(x_t, \lambda_t | y^{obs}_{1:t-1}\right),$$

where C is a normalization constant and the other two factors are the likelihood function, to which we assign a known distribution, and the forecast pdf, computed in (3), respectively. The analysis step essentially consists in a reinitialization of the system state variables and of the parameters given the forecast and the observations.

In the SIR algorithm the forecast and filtering pdfs are approximated using an ensemble of N random samples (also called particles), $\{x^{(i)}_t, \lambda^{(i)}_t\}$, $i = 1, \ldots, N$, with associated weights $\{\omega^{(i)}_t\}$, $i = 1 \ldots, N$:

$$\begin{aligned} p\left(x_t, \lambda_t | y^{obs}_{1:t-1}\right) &\approx \sum_{1=1}^{N} \omega^{(i-)}_t \delta\left(x_t - x^{(i-)}_t\right) \delta\left(\lambda_t - \lambda^{(i-)}_t\right), & (4) \\ p\left(x_t, \lambda_t | y^{obs}_{1:t}\right) &\approx \sum_{1=1}^{N} \omega^{(i+)}_t \delta\left(x_t - x^{(i+)}_t\right) \delta\left(\lambda_t - \lambda^{(i+)}_t\right), & (5) \end{aligned}$$

where $\delta(\cdot)$ is the Dirac delta function, and superscripts '$-$' and '$+$' denote the realizations before and after the update, respectively. The SIR algorithm starts by assigning uniform weights to the N realizations of the ensemble.

The Monte Carlo discretization reduces the forecast step to the propagation in time of the ensemble members using the system dynamics and, in the update step, new weights are calculated recursively, by means of the likelihood function, as:

$$\omega_t^{(i)} = C\omega_{t-1}^{(i)} p(y_{1:t}^{obs}|x_t^{(i-)}, \lambda_t), \tag{6}$$

where C is a normalization constant. To avoid the ensemble deterioration phenomenon [41], resampling is performed when $N_{eff} < 0.5N$, where N_{eff} is the effective ensemble size, evaluated as:

$$N_{eff} = \left[\sum_{i=1}^{N} (\omega_t^{(i)})^2\right]^{-1},$$

and is representative of the number of realizations that have non-negligible weights. We adopt the systematic resampling method [42], to duplicate samples with large weight and discard samples with negligible weight. The resampling procedure maintains the ensemble size equal to N by generating new members using parameters drawn from the posterior distribution and assigning to them uniform weights. The duplicated realizations will then differentiate in the following forecast step. If the resampling step does not occur, i.e., all the particles have sizable weights, then $x_t^{(i+)} = x_t^{(i-)}, \lambda_t^{(i+)} = \lambda_t^{(i-)}$ and only the weights are changed according to (6), yielding an effective weighted distribution given by (4) and (5).

2.2. Iterative parameter estimation

Since the resampling step is a reinitialization of the system state variables at an observation time, it is convenient to use this step to sample new realizations from the posterior pdf of the parameters. Let $\{\hat{\lambda}_t^{(i)}\}$, $i = 1, \ldots, N$ be the parameter values of the realizations after the resample. Most of these parameters are equal, the number of different values corresponding to the number of realizations that have non-negligible weights. Maintaining these values for the parameter update, i.e. $\lambda_t^{(i+)} = \hat{\lambda}_t^{(i)}$, may yield an impoverishment of the ensemble with the consequence that the posterior distribution is not adequately explored and erroneous parameter estimations may be identified. This can be exemplified in the case that only one realization is duplicated after the resample. In this case the posterior distribution collapses in one single value that cannot change in the subsequent updates. To guarantee a good performance of the filter it is then necessary to perturb the duplicated parameters to effectively explore the relevant pdf. Moradkhani et al. [28] propose a perturbation of the parameters with independent additive Gaussian variates, $\lambda_t^{(i+)} = \hat{\lambda}_t^{(i)} + \xi_t^{(i)}$, $\xi_t^{(i)} \sim N(0, Var(\lambda_t^{(i-)}))$, while [43, 44] use a Markov-Chain sampling of the parameters with the computation of the Metropolis ratio to accept or eventually reject the sampled values. While the first approach requires a large number of realizations, the second strategy incurs in increased computational effort due to the repetition of the forecast step necessary for the computation of the Metropolis ratio. Here we propose to sample the updated parameters from a probability distribution that maintains the initial structure, but employing the moments updated with the ensemble statistics. For example, assuming an initial distribution defined only by the first and second moments (e.g., uniform, normal, log-normal distributions), the proposed scheme updates the expected value μ_{λ_t} and the coefficient of variation cv_{λ_t} on the basis of the prior $\{\lambda_t^{(i-)}\}$ and the resampled $\{\hat{\lambda}_t^{(i)}\}$ parameters. To this aim, we impose that the expected value of the new distribution be given by the mean of the resampled parameters:

$$\mu_{\lambda_t} = E[\hat{\lambda}_t^{(i)}], \tag{7}$$

and the coefficient of variation be given by the maximum between the coefficient of variations of the forecasted and the updated parameters,

$$cv_{\lambda_t} = s \cdot \max\left(cv_{\lambda_t^{(-)}}, cv_{\hat{\lambda}_t}\right), \tag{8}$$

where s is a tuning coefficient used to force a gradual reduction of the variance of the distribution (typically s=0.9) and the use of the maximum value avoids the fast collapse of the filter when only a few realizations are resampled. The sequence of posterior parameter distributions obtained with this procedure needs several updates to converge and hence we iterate the filtering procedure by cyclic repetition of the assimilation interval until the resampling step is no longer performed at any update of the period. This stopping criterion ensures that no further progresses are obtained by continuing the iterations. A more computationally savvy approach would be to stop on the basis of average residual or parameter update metrics. At each restart of the filtering process (external iteration) the mean and variance of the prior distribution of the parameters is updated by:

$$\begin{aligned}
\mu_{\lambda_0}^{k+1} &= \frac{1}{n_t}\sum_{t=1}^{n_t} \mu_{\lambda_t}^{k}, \\
cv_{\lambda_0}^{k+1} &= \frac{1}{n_t}\sum_{t=1}^{n_t} cv_{\lambda_t}^{k},
\end{aligned}$$

where n_t is the number of updates in each S-DA cycle (k-th external iteration). Instead of restarting the S-DA procedure with the posterior distribution at the previous S-DA cycle, we use a "mean posterior disitribution" to reduce the effect of the initial bias on the parameter estimation. The procedure is illustrated schematically in Figure 1.

3. Evolution and Observation models of water infiltration and ERT

In this study we are interested in applying the S-DA method to a coupled hydro-geophysical model. The evolution model (1) describes the soil moisture dynamics in the vadose zone and ERT observations are used to update system state and parameters by means of a geophysical electrical current flow observation model (2).

3.1. Evolution model

We use Richards' equation to describe the infiltration process in a variably-saturated isotropic porous medium:

$$S_s S_w(\psi) \frac{\partial \psi}{\partial t} + \phi \frac{\partial S_w(\psi)}{\partial t} = \vec{\nabla} \cdot \left[\boldsymbol{K}_s K_r(\psi) \left(\vec{\nabla}\psi + \eta_z \right) \right] + q, \qquad (9)$$

where S_s is the elastic storage term, S_w is water saturation, ψ is water pressure, t is time, ϕ is the porosity, $\boldsymbol{K}_s$ is the saturated hydraulic conductivity tensor, K_r is the relative hydraulic conductivity, $\eta_z = (0, 0, 1)^T$ with z the vertical coordinate directed upward and q is a source/sink term. The saturated hydraulic conductivity is modeled as a diagonal matrix and its components K_x, K_y and K_z are the saturated hydraulic conductivities along the coordinate directions x, y and z, respectively. Equation (9) is highly nonlinear due to the pressure head dependencies of saturation and relative hydraulic conductivity. These constitutive functions are modeled using the characteristic

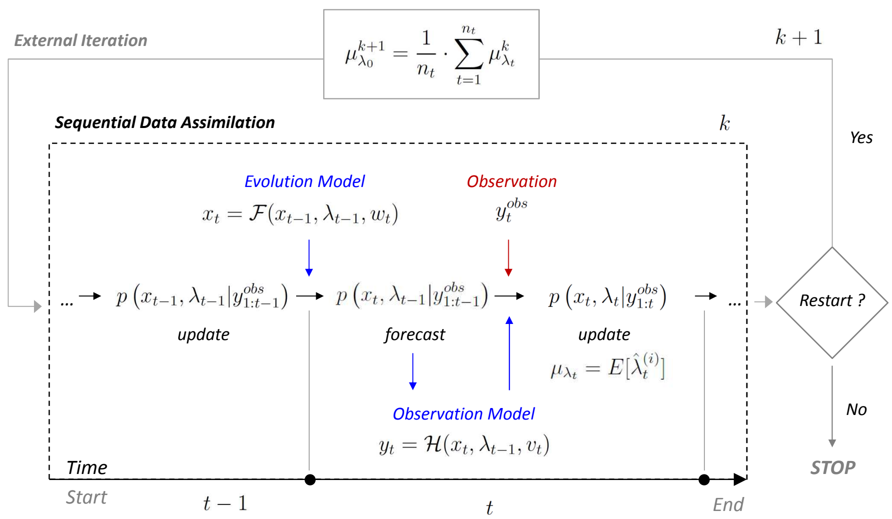

Figure 1: Scheme of the iterative particle filter method (modified from [45]). The data assimilation cycle starts with a distribution of the system state at time $t-1$ which is used by the evolution model to provide a forecast at time t. The forecast state is converted by the observation model into a forecasted observation which is combined with the field observation y_t to produce the update at time t. When all the available data are assimilated, the data assimilation cycle is restarted (k-th external iteration) until convergence of the model parameter λ_t (see main text for details).

relations proposed by [46]:

$$S_w(\psi) = \begin{cases} (1 - S_{wr})(1 + \beta_\psi)^{-m} + S_{wr} & \psi < 0, \\ 1 & \psi \geq 0, \end{cases} \tag{10}$$

$$K_r(\psi) = \begin{cases} (1 + \beta_\psi)^{-m/2} \left[(1 + \beta_\psi)^m - \beta_\psi^m\right]^2 & \psi < 0, \\ 1 & \psi \geq 0, \end{cases} \tag{11}$$

where S_{wr} is the residual water saturation, $\beta_\psi = (\psi/\psi_s)^\alpha$, ψ_s is the capillary or air entry pressure, α is a constant and $m = 1 - 1/\alpha$, with $1.25 < \alpha < 6$. Equation (9) is numerically solved using the subsurface module of the CATHY model (CATchment HYdrology [47]), a linear tetrahedral finite element method with backward Euler scheme with adaptive time stepping and Newton-like iterations for the solution of nonlinear system [48]. The system state vector x_t of (1) collects the nodal pressure head ψ at simulation time t. The nonlinear function $\mathcal{F}$ is a formal representation of the numerical solver and comprises a number of time steps to advance within the assimilation interval $[t-1, t]$. The stochastic noise w_t, kept constant during the forecast step, represents model uncertainty and is generally specified by a normal or lognormal distribution of the parameters.

3.2. Observation model

We monitor the infiltration process with ERT measurements. ERT emits direct current (DC) from evenly spaced electrodes installed at the soil surface and monitors the electrical potential differences at other locations. The DC injection pairs are moved sequentially to generate a number of electrical potential fields. Using moisture content-resistivity relationships (e.g.., Archie's Law [49, 50]) and assuming that changes in conductivity correspond to changes in moisture content, the water flow in the vadose zone can be monitored [17, 38, 51]. The intensity of the electrical potential field Φ induced in the soil by the input current can be modeled as [51]:

$$-\vec{\nabla} \cdot \left[\kappa\left(S_w\right) \vec{\nabla}\Phi\right] = I\left[\delta\left(\vec{r} - \vec{r}_{S+}\right) - \delta\left(\vec{r} - \vec{r}_{S-}\right)\right], \tag{12}$$

where κ is the scalar electrical conductivity of the bulk (porous medium plus contained fluid), I is the applied current, δ is the Dirac delta function, and $\vec{r}_{S+}$ and $\vec{r}_{S-}$ are the current source and sink electrode position vectors, respectively. The soil electrical conductivity is related to saturation according to the following petrophysical relationship that is derived from Archie's law [6]:

$$\kappa\left(S_w\right) = \kappa\left(t_0\right)\left(\frac{S_w\left(t\right)}{S_w\left(t_0\right)}\right)^n, \tag{13}$$

where $S_w(t_0)$ and $\kappa(t_0)$ are the initial water saturation and the corresponding initial electrical conductivity of the soil, respectively, and n is a dimensionless parameter generally calibrated in the lab using soil samples. Since water saturation varies during the infiltration process, the induced electric field is time dependent. Let y_t^{obs} be the vector collecting the electrical potential differences that are observed at the measurement electrodes at time t. Equations (10)-(11), (12) and (13) imply that there exists a nonlinear relation between the water pressure in the soil and the electrical potential differences at all electrodes. In fact, van Genuchten relations (10)-(11) and Archie's law (13) allow us to calculate the soil electrical conductivity field from the water pressure. Equation (12) is solved numerically using a three-dimensional linear finite element solver. In order to avoid boundary effects on the simulated electrical potential, the model domain used to simulate the infiltration experiment for both the hydrological and DC current models is enlarged in the three spatial directions to accommodate the geophysical simulations. The solution of (12) gives the electrical potential differences $y_{t,i}$, $i = 1, \ldots, N_{obs}$, at the N_{obs} electrode positions to be compared to the corresponding field measurements y_t^{obs}. The general observation model of equation (2) becomes $y_t = \mathcal{H}(\psi_t)$, where $\mathcal{H}$ embeds the nonlinear relation between the soil moisture and the electric potential. The observation y_t^{obs} can then be related to the measurement model using the measurement uncertainties as:

$$y_t^{obs} = y_t (1 + v_t),$$

where v_t is the observation error, modeled as an unknown realization of a normal random variable with zero mean and standard deviation equal to σ_y. The term v_t incorporates both measurement errors and observation model uncertainties. From the previous equation and the probability distribution of v_t we can now explicitly derive the expression for the likelihood function $p(y_t^{obs}|x_t)$, which in the case of a normal distribution becomes:

$$p\left(y_t^{obs}|x_t\right) = C \cdot exp\left[-\frac{1}{2}\sum_{j=1}^{N_{obs}}\left(\frac{y_{t,j}^{obs} - y_{t,j}}{\sigma_y y_{t,j}}\right)^2\right],$$

where C is a normalization constant. This pdf is estimated from the MC ensemble, hence completing the overall inversion algorithm.

4. Experimental Results

The performance of the proposed approach was tested on a controlled infiltration field experiment. First, using the geometry of the real case study,

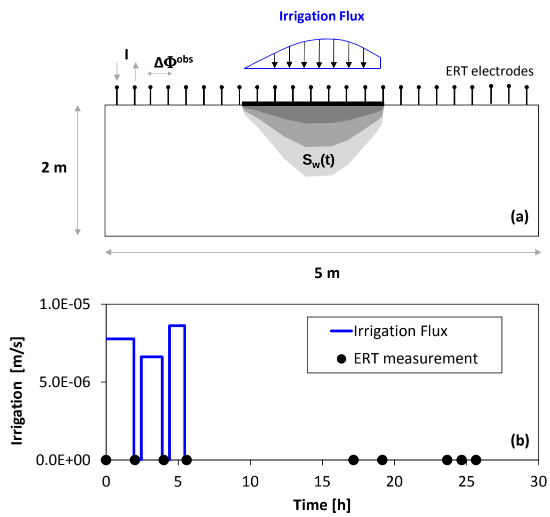

Figure 2: Schematic representation of the system geometry (a) and time-behavior of the infiltration flux rates imposed at the surface boundary (b). Black dots indicate the time of ERT measurements.

Table 1: Time invariant model parameters

Parameter	Description	Unit	Value	Reference
Evolution model				
ϕ	Soil porosity	-	0.33	[52]
S_s	Elastic storage	m^{-1}	5.0E-04	Assumed
S_{wr}	Residual saturation	-	0.003	[53]
ψ_r	Capillary pressure	m	-0.185	[53]
α	VG model parameter	-	2.0	[53]
Observation model				
n	Archie's law parameter	-	1.27	[52]
$S_w(t_0)$	Initial value of S_w	-	0.21	Field data
$\kappa(t_0)$	Initial value of κ	$\mathrm{S\ m}^{-1}$	7.69E-04	Field data

a synthetic problem is designed in order to assess the convergence properties of the developed scheme, then, the real field experiment is simulated.

The controlled infiltration experiment is described in [54] and is similar to a previous experiment discussed by [55]. The experimental site is located in Grugliasco (Turin, Italy), nearby the campus of the Agricultural Faculty of the University of Turin. It is characterized by a regular stratigraphic sequence of sandy soil composed mainly of eolic sands with low organic content [52, 56]. In the unsaturated zone, sand grains are relatively homogeneous with a median diameter (d_{50}) of 200 μm and porosity of $\phi = 0.33$ forming a homogeneous and isotropic soil in the horizon interested by the infiltration process [52]. The water table is located approximately 20 m below the surface and the vadose zone is not influenced by the underlying aquifer. A line of sprayers was used to wet an area of about 3 m$\times$20 m for 6 hours using variable in time irrigation rates (shown in Figure 2(b)).

The infiltration front was monitored by means of both ERT and GPR WARR surveys [54] along a cross section of the irrigated area. ERT was performed in time-lapse mode using a dipole-dipole configuration, using 24 electrodes placed on the soil surface with a regular spacing of 0.2 m. ERT data were acquired before irrigation (background ERT), during short intervals within the irrigation period, and after the end of irrigation for the following 24 hours. The exact timings of the ERT acquisitions used in the data assimitation procedure (i.e. during and after irrigation) are shown as bullets in Figure 2(b).

Soil samples at different depths were collected and used to obtain laboratory estimates of the hydrological parameters S_s, ϕ, α, ψ_s, and S_{wr}, as well as Archie's law constant n. Initial volumetric water content was estimated from GPR measurements at 0.07 m^3 m^{-3}, corresponding to an initial water saturation $S_w(t_0) = 0.21$, while background ERT measurements were used to determine the initial soil electrical conductivity $\kappa(t_0) = 7.69 \times 10^{-4}$ S m^{-1}, corresponding to a resistivity of 1300 Ω m. This value is in accordance with Archie's law parameter calibrated during the laboratory experiments [52]. The values of these parameters are reported in Table 1.

Inverted resistivity data, obtained from the uncoupled approach developed by [4], revealed that irrigation was not uniformly distributed in the direction orthogonal to the sprinkler line, probably due to the presence of wind [54]. This was taken into account in order to properly define the top boundary conditions and the irrigation flux was thus modeled with a Gaussian distribution centered at 2.5 m (top boundary), with variance equal to 0.6 m, both values calculated such that the total flux equals the real irrigation rate.

The model of the field experiment is developed using a vertical cross-section orthogonal to the irrigation line, whose schematic representation is illustrated in Figure 2(a). For the hydrologic simulation, no-flow boundary conditions (BCs) were set all over the model domain, except for the top boundary where the irrigation rate was imposed as a Neumann flux. Spatially varying input infiltration is considered as a potential rate, and actual infiltration is evaluated based on system state condition allowing the switching between Neumann and Dirichlet BCs in the case of ponding [47].

The finite element grid of the hydrologic model consists of 9792 nodes and 49500 elements while the stationary geophysical model was solved on an enlarged mesh characterized by 21240 nodes and 112404 elements.

4.1. Synthetic case

In the synthetic cases, a forward simulation of both the hydrological and the ERT models with pre-imposed parameters was used to generate the true state and the ERT measurements. We are interested in identifying saturated homogeneous or spatially heterogeneous hydraulic conductivity, simulated with a lognormal distribution to ensure positivity of the parameters values [e.g. 57, 58]. All other model parameters are based on the values used in the field case study as listed in Table 1. The synthetic dataset of ERT observations was generated by the coupled hydro-geophysical forward model assuming the same dipole-dipole configuration of the field experiment. It was then used to constrain the particle filter simulations assuming different levels of measurement errors (σ_y = 5 - 20%).

The convergence of the proposed coupled inversion method is tested by looking at the behavior of a number of error statistics. The discrepancy between measured and simulated observations (electrical potential at the electrodes) is evaluated in terms of ensemble mean relative error (ϵ_y), maximum relative error ($\epsilon_{y,max}$) and root mean square error ($RMSE_y$):

$$
\begin{aligned}
\epsilon_y &= \frac{1}{N}\sum_{i=1}^{N}\left[\frac{1}{N_{obs}}\sum_{j=1}^{N_{obs}}\frac{|y_{t,j}^{i,\Phi}-y_{t,j}^{obs}|}{|y_{t,j}^{obs}|}\right] \\
\epsilon_{y,max} &= max_i\left\{max_j\left\{\frac{|y_{t,j}^{i,\Phi}-y_{t,j}^{obs}|}{|y_{t,j}^{obs}|}\right\}\right\} \\
RMSE_y &= \frac{1}{N}\sum_{i=1}^{N}\left[\frac{1}{N_{obs}}\sqrt{\sum_{j=1} N_{obs}\frac{|y_{t,j}^{i,\Phi}-y_{t,j}^{obs}|^2}{|y_{t,j}^{obs}|^2}}\right]_i
\end{aligned}
$$

We also look at the L_2-norm of the error ϵ_ψ between the true and the simulated system state values, soil water pressure head, named the pressure error:

$$\epsilon_\psi = \|\bar{\psi}_t - \psi_t^{true}\|_2$$

where $\bar{\psi}_t$ is the ensemble mean pressure field at time t. For all the simulations we require a fixed number (8) of iterations chosen so that convergence is reached within a reasonable computational time and a reliable assessment of error statistics is obtained. The use of one of the stopping criteria proposed in section 2.2 would yield faster convergence in all test cases.

4.1.1. Homogeneous test case

In this test case, an isotropic and homogeneous soil with hydraulic conductivity equal to $\boldsymbol{K}_s = 10^{-5}$ [m s^{-1}] was employed. The saturated hydraulic conductivity tensor is thus the only unknown parameter $\lambda_t = \{\boldsymbol{K}_s\}$ with $K_x = K_y = K_z$ (homogeneous and isotropic soil).

A preliminary sensitivity analysis on the ensemble size carried out with $N = 20, 50, 100$ suggests that 20 particles are enough for this case study to obtain reliable estimates. Hence, a value $N = 20$ particles is used to test the performance of the method with the different measurement errors. Figure 3 reports the convergence results in terms of both parameter values (left panel) and errors (right panel). To better illustrate the behaviour of the pdf of the hydraulic conductivity during the iterative procedure, the simulation results obtained with 100 particles are also shown (Figure 4).

The hydraulic conductivity estimated by the iterative particle filter method is shown to converge to the true value $\boldsymbol{K}_s^{true}$ as the number of updates is sufficiently large (Figure 3). The number of updates necessary for convergence

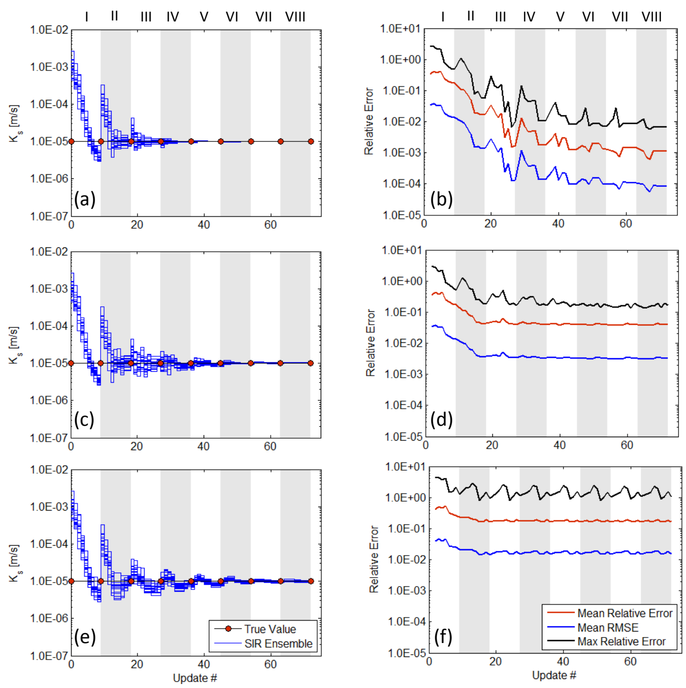

Figure 3: Synthetic test case results: convergence of the hydraulic conductivity (a,c,e) and relative errors between true and simulated observations (b,d,f). Mean relative error (ϵ_y), Mean $RMSE_y$ and Maximum Relative error ($\epsilon_{y,max}$) are shown. The performance of the method for different measurements error is illustrated: (a,b) $\sigma_\Phi = 5\%$ with measurements not randomly perturbed, (c,d) $\sigma_\Phi = 5\%$, and (e,f) $\sigma_\Phi = 20\%$ with randomly perturbed measurements. Red dots indicate the true value of $\boldsymbol{K}_s$. The roman numerals indicate the external iteration step. Each external iteration consists of 8 SIR updates

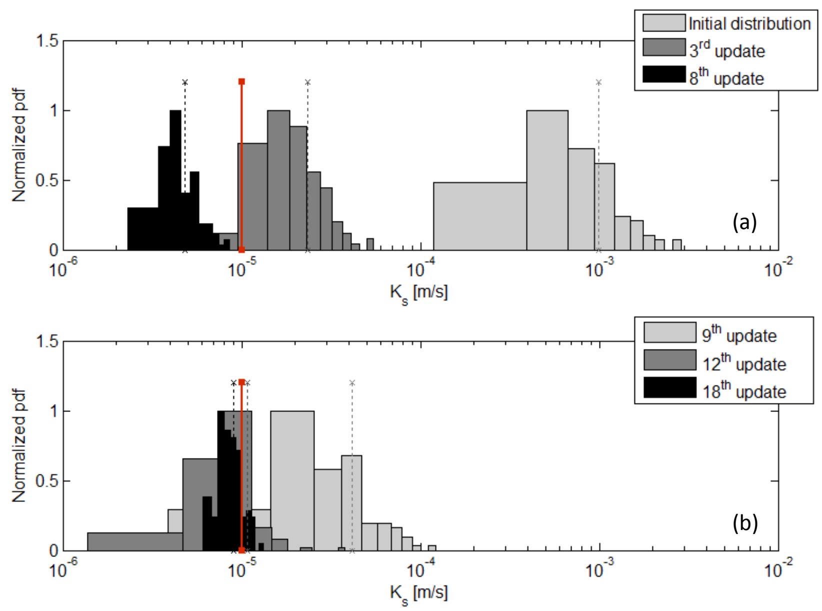

Figure 4: Synthetic test case results: pdf of the hydraulic conductivity normalized on the maximum value of the pdf. Panel (a) and (b) refer to the first and second external iteration of the SIR method, respectively. The simulation was run with an ensemble size N=100. Dotted lines indicate the ensemble mean and the red line indicates the true value of $\boldsymbol{K}_s$.

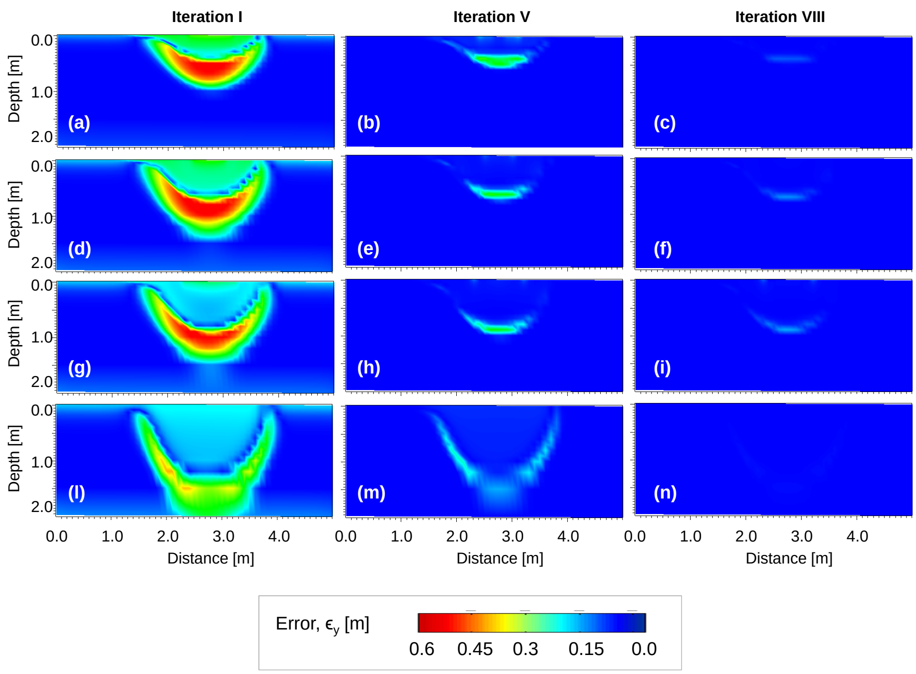

Figure 5: Spatial distribution of the error ϵ_ψ, representing the discrepancy between simulated (ensemble mean) and true system state (pressure field).

depends on the measurement error: when the true observations are assimilated, i.e. when the observations are not randomly perturbed, the method approaches $\boldsymbol{K}_s^{true}$ after four iterations (Figure 3a) but for increasing noise, more iterations are needed to achieve convergence. As a matter of fact, for $\sigma_{\Phi} = 5\%$ and 20% the estimated value $\mu_{\lambda_{t,k}}$ keeps oscillating until the 6^{th} and 7^{th} external iteration, respectively (Figure 3(c) and Figure 3(e)). The convergence speed depends on σ_{Φ}, observing slower convergence for higher noises. The results demonstrate that the traditional particle filter (i.e. the non-iterative approach) may provide a biased estimate of the model parameter unless larger ensemble sizes are used. This is highlighted in Figure 4 where the pdf of the hydraulic conductivity at different updates of the first and second iterations are shown. If the initial guess of the model parameter is overestimated, the predicted value at the end of the first iteration (8^{th} update in Figure 4(a)) is underestimated. This is due to the fact that the particle filter has to correct the model parameter more than necessary to balance the bias on the predicted state during the initial updates. For example, a higher initial estimate of $\boldsymbol{K}_s$ corresponds to a higher infiltration capacity and thus causes an over-estimated total infiltrated water, with a corresponding over-estimation of the front speed. Hence, at later times, the inversion procedure must identify an under-estimated $\boldsymbol{K}_s$ to accommodate the slower observed saturation front depth. As a result, the pdf of the parameter is shifted further than necessary on the opposite direction of the initial guess. The iterative approach allows the filter to "forget" the initial bias and converge more efficiently to the true parameter (Figure 4(b)). The results in Figure 5 show that the error ϵ_{ψ} develops at the edge of the infiltration front where sensitivities are highest. The iterative procedure successfully reduces the discrepancy between simulated and true system state and the restart is shown to be fundamental to achieve negligible errors. The traditional SIR method corrects also the system state after each update but errors up to 0.6 m (in term of predicted pressure head) are still observed at the end of the first iteration of the sequential procedure. The iterated approach allows instead a reduction of the error ϵ_y down to negligible values ($\epsilon_y < 10^{-3}$ m). The synthetic simulations confirmed that the particle filter is an efficient method to update the system state and the iterative procedure is shown to be essential to provide precise estimates of the model parameters at lower computational effort.

4.1.2. Heterogeneous test case

The ability of the proposed methodology to estimate multiple model parameters is investigated. We consider the same infiltration experiment, now characterized by an isotropic heterogenous soil (Figure 6(a-b)). The model domain is divided into four zones with different hydraulic conductivities (thus providing four unknown model parameters). The physical setting in Fig. 6(a) is not intended to represent typical field conditions but aims to provide a simple setup generating both vertical and lateral infiltration patterns to test the proposed approach in a truly multidimensional heterogeneous setting. The results of the iterative SIR scheme, shown in Figure 6(c-d), demonstrate that this approach successfully estimates multiple model parameters. To assess the sensitivity to the initial condition, we simulated the same test problem with different values of the initial guess. Figure 7 reports an example of the identification results in the case of underestimated initial solutions. We

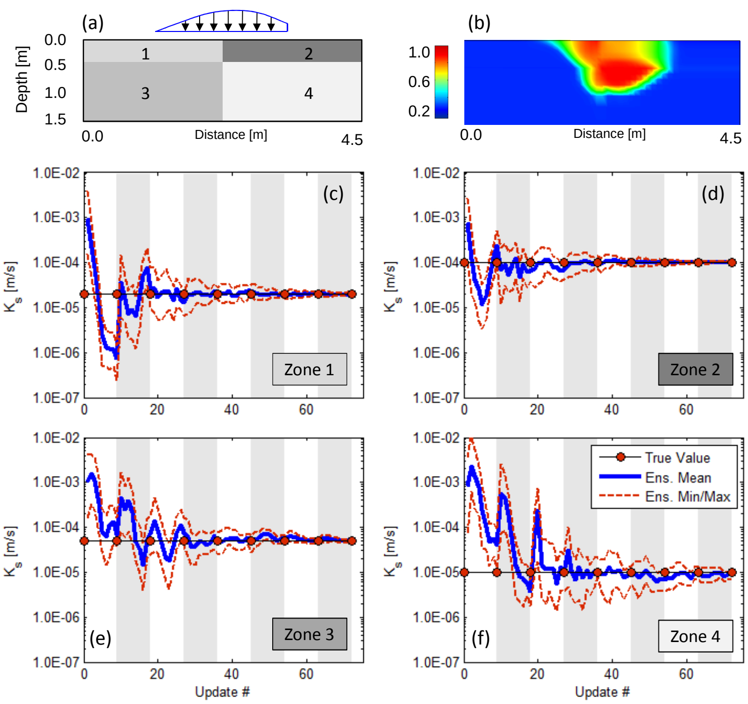

Figure 6: Heterogeneous test case results: (a) conceptual model of the model domain (divided into 4 zones with different soil properties) and (b) the simulated soil saturation at $t = 5.5h$. Convergence of the hydraulic conductivities of the four zones is shown in panels c-f. The results are relative to $\sigma_{\Phi} = 5\%$ with randomly perturbed measurements.

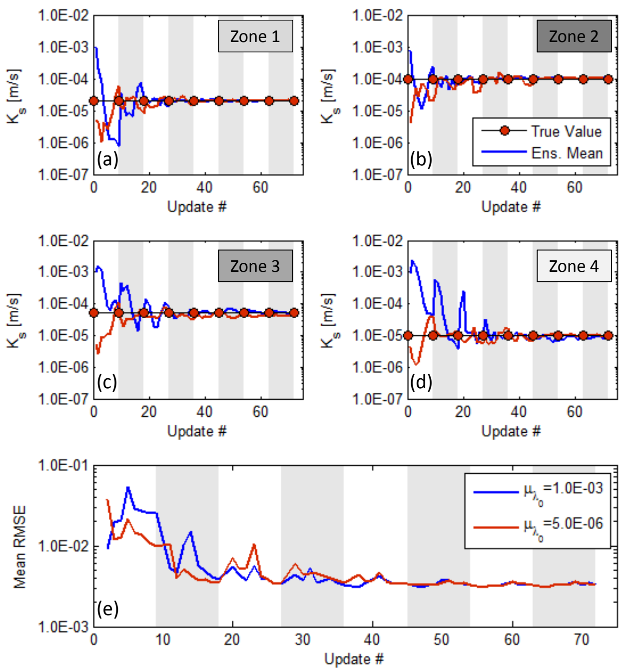

Figure 7: Heterogeneous test case results: convergence of the hydraulic conductivities (ensemble mean values) of the four zones (a-d) and mean RMSE (e) for different initial values μ_{λ_0}. The results are relative to $\sigma_{\Phi} = 5\%$ with randomly perturbed measurements.

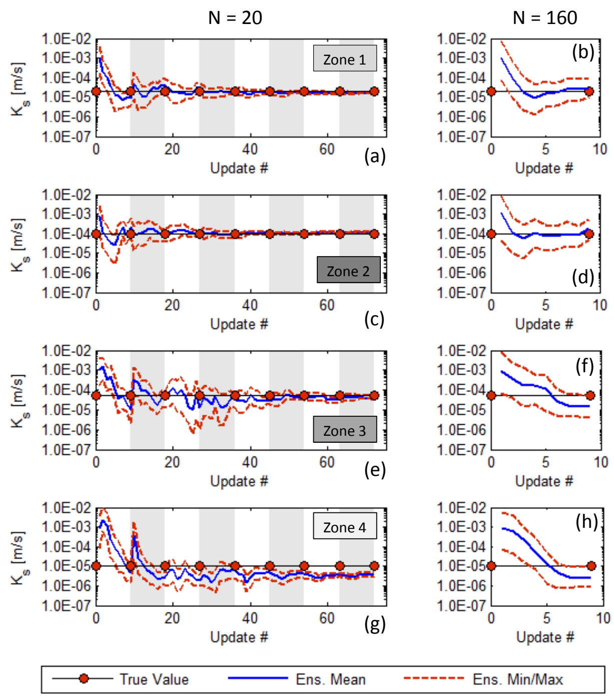

Figure 8: Heterogeneous test case results: comparison of the iterative approach ($N = 20$) with a non-iterative simulation with ensemble size $N = 160$. The convergence of the four hydraulic conductivities for the iterative (panels a,c,e,g) and non-iterative (panels b,d,f,h) cases is illustrated (runs with $\sigma_{\Phi} = 20\%$ and randomly perturbed measurements).

notice that the behavior of the iterative SIR method is qualitatively similar independently on the initial solution, thus confirming the reliability of the proposed approach.

We note that the identification is practically achieved after four iterations, for a total of 80 forward model runs. At later iterations the identified values of zones 3 and 4 display small oscillations whose amplitude seem to decrease as the scheme progresses (Figure 6(e-f)). This is likely due to the fact that both zones 3 and 4 receive information from the infiltration experiment at later times. At the first 4 observation times the true infiltration front is shallower than the material interface, and only the last 4 measurements contribute information towards the identification of hydraulic conductivity of zones 3 and 4.

To test the improvements obtained by our proposed iterative method with respect to standard (non iterative) DA methods, we solve the same problem with a one-iteration SIR approach but with an ensemble size $N = 160$. This value corresponds the same number of forward model runs used in the previous simulations using (pre-fixed) eight iterations. We perform this comparison for the case of $\sigma_{\Phi} = 20\%$ and randomly perturbed measurements.

The convergence results of the iterative and non-iterative procedures for this case are compared in Figure 8. The iterated simulation converges to the correct hydraulic conductivities of zones 1, 2 and 3, and only a small discrepancy persists in the estimation of $\boldsymbol{K}_s$ in zone 4. The value of this bias is consistent with the 20% measurement uncertainty, implying that the inverse procedure has arrived at the correct solution. On the contrary, the results for the non-iterative SIR show a bias in the identification of the parameters of zones 3 and 4 that is larger than the variability dictated by the measurement error. The corresponding ensemble means underestimate the true values, reflecting the earlier observation that starting from a large $\boldsymbol{K}_s$ leads to an underestimation of the parameter value. The final posterior distributions of the parameters have a higher ensemble variance than the corresponding iterative-results, yielding an uncertain characterization of the soil structure. The non-iterative SIR procedure shows a parameter distribution with strong variations during the assimilation, corresponding to a large variance of the posterior distribution.

4.2. Field experiment

The results of the field data inversion are shown in Figure 9. The assimilation of ERT measurements provides similar results to the synthetic test case, thus confirming the reliability of the method. The iterative particle filter is shown to converge to a value of hydraulic conductivity $\boldsymbol{K}^*$ which is independent to the initial guess μ_{λ_0}. As a matter of fact, starting from $\mu_{\lambda_0} = 10^{-3}$ ms^{-1} the method provides a final estimate $\boldsymbol{K}^* = 8.9 \times 10^{-6} \pm 3.6 \times 10^{-7}$ ms^{-1} and starting from $\mu_{\lambda_0} = 10^{-7}$ ms^{-1}, the final estimate is $\boldsymbol{K}^* = 9.8 \times 10^{-6} \pm 2.9 \times 10^{-7}$ ms^{-1}. Note that in both cases the initial guess is two orders of magnitude away from the final estimate and the two final intervals for the identified parameter value are overlapping. It must be emphasized that the method does not provide just an estimate of hydraulic conductivity but a full probability distribution of the estimate. As shown by the synthetic test, in the case of large measurement noise, the relative errors slightly decrease during the first updates and quickly stabilize. The residual errors are larger than observed in the synthetic test case

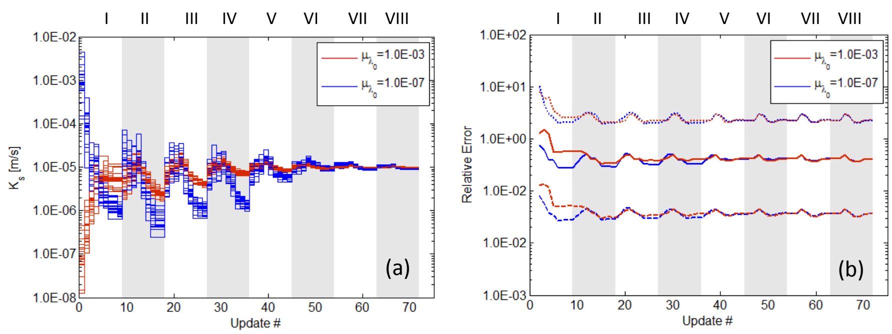

Figure 9: Field experiment results: convergence of the hydraulic conductivity (a) and relative errors (b) for different initial values of hydraulic conductivity μ_{λ_0}. The roman numerals at the top of the panels indicate the external iteration count. Mean relative error (ϵ_y), Mean $RMSE_y$ and Maximum Relative error ($\epsilon_{y,max}$) are shown.

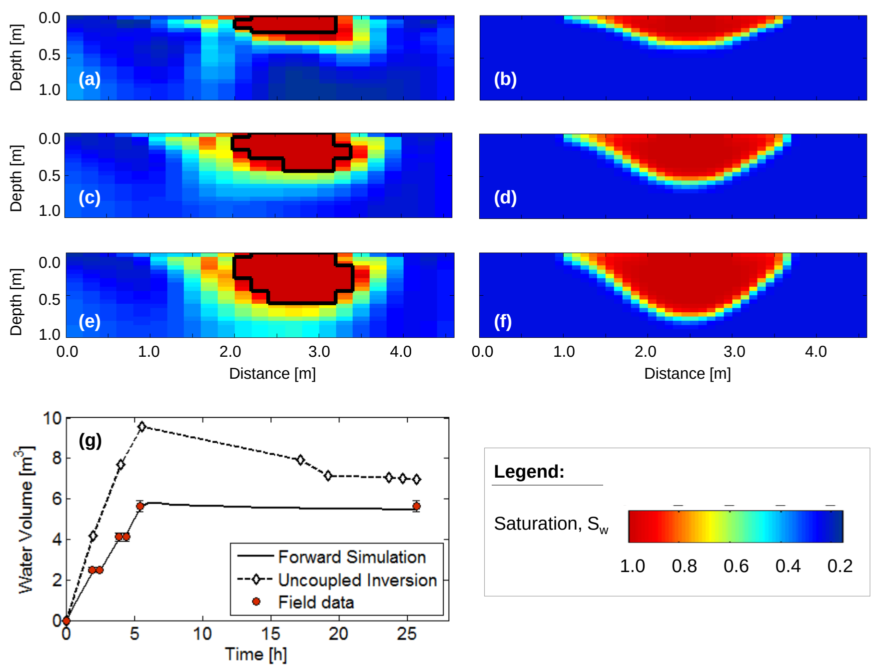

Figure 10: Time-lapse soil saturation estimated by uncoupled inversion (a,c,e) and by the forward simulation with the hydraulic conductivity estimated by the coupled approach (b,d,f). The results are shown at (a,b) $t = 2h$, (c,d) $t = 4h$, and (e,f) $t = 5.5h$. The black contour indicates the area where uncoupled inversion provides unphysical saturation estimates ($S_w > 1$). Mass balance (g): the forward simulation (black line) matches the volume of water injected at the site (red circles with a 5% error bar) while the estimate from uncoupled inversion of ERT data overestimates the mass of water in the system.

thus indicating a bias due to external factors not accounted for in the model setup. The hydraulic conductivity estimated by the iterative particle filter method is shown to converge to the $\boldsymbol{K}^*$ value. However, the reliability of the estimate has to be proven. For this purpose, a forward hydrologic simulation is run with $\boldsymbol{K}_s = \boldsymbol{K}^*$ and the results are compared with field observations (Figure 10). The robustness of the estimated parameter is confirmed by the spatial agreement of simulated soil moisture fields obtained by the coupled and uncoupled inversion procedures (Figure 10(a-f)) and by the excellent agreement between the amount of injected water and the predicted mass balance (Figure 10(g)). Further comparison between the forward simulation and field data are presented in [54] where the simulated infiltration is shown to match the front depth estimated by the GPR survey. The discrepancy between the simulation and the time-lapse saturation estimated by uncoupled inversion increases for increasing front depth. As a matter of fact the resolution of traditional ERT inversion decreases with depth and, given the electrode configuration used in this study, the inverted resistivity is not reliable for depth higher than 1 m. In addition, the conversion of inverted resistivity to soil saturation by Archie's law (calibrated in the lab) provided regions of $S_w > 1$ (black contour in Figure 10). Even though these regions can be corrected empirically to ensure a consistent saturation field (according to common practice in geophysical applications anyway) the uncoupled approach over-estimates the total water present in the system at any time (Figure 10). Therefore, while the forward simulation provides a full conservation of mass, the traditional inversion approach provides a good qualitative description of the physical process but does not ensure a correct mass balance

(Figure 10g).

5. Discussion

The results presented in this paper demonstrate the accuracy and robustness of the proposed iterative methodology and highlight the weaknesses of both, uncoupled ERT inversion and traditional particle filter applications with ERT data. As shown in Figures 3, 4, and 8 for the synthetic test cases and in Figure 9 for the field simulations, a single iteration of the particle filter method does not provide a reliable estimate of the soil hydraulic conductivity. To verify this hypothesis, we use as initial guess the parameter value $\mu_{\lambda_0} = 10^{-3}$ m s^{-1} and then employ the identified parameter μ_{λ_8} estimated at the end of the first iteration to run a forward simulation of the infiltration experiment. In this case, the irrigation intensity is found to be higher than the infiltration capacity, thus leading to surface ponding not observed at the site during the experiment. Therefore, if the particle filter is used to estimate the model parameters without enough updates to ensure convergence, the method may lead to wrong predictions of the system dynamics. The results of our simulations further show that a non-iterative SIR approach with a large ensemble is not fully capable of performing a correct identification, suggesting that the iterative approach is computationally more efficient for solving the problem of interest.

The proposed coupled hydro-geophysical modeling framework presents the following advantages compared to more traditional approaches: (1) a forward geophysical model is used and the inversion of the geophysical data is avoided thus guaranteeing physical consistency with the hydrologic quantities; (2) the sequential approach provides a dynamic correction of the simulated system state, thus correcting intrinsic model errors (i.e. unknown initial condition), with relatively small compuational requirements; (3) the data assimilation approach is particularly interesting for field applications where the geophysical measurements can be affected by external factors (e.g. soil evaporation, a rainfall event during the geophysical survey, etc.) that can be easily included in the hydro-geophysical modeling framework; (4) the filtering approach describes quantitatively both model and observation errors, and provides the probability density functions of both system state and model parameters.

6. Conclusions

A sequential Bayesian approach for coupled hydro-geophysical assimilation of ERT measurements in a variably saturated flow model is presented. An innovative iterative approach is proposed to achieve accurate identification of the model parameters. The robustness of the methodology is tested on spatially homogeneous and heterogeneous synthetic test cases and validated on a field infiltration experiment. We show that the new approach has several advantages compared to uncoupled inversion and traditional sequential data assimilation techniques. In particular the iterative particle filter provides accurate parameter estimation as opposed to traditional SIR that may lead to biased results. Further work will focus on testing the methodology for the estimation of multiple and spatially varying parameters (e.g. Archie's law, retention curves, heterogeneous soil, etc.).

7. Acknowledgments

This study was funded by the University of Padova, Italy, within the Research Programme “GEO-RISKS: Geological, morphological and hydrological processes: monitoring, modeling and impact in the north-eastern Italy”, WP4. The authors would like to acknowledge partial funding from the EU FP7 project CLIMB (“Climate Induced Changes on the Hydrology of Mediterranean Basins - Reducing Uncertainty and Quantifying Risk”) and the Italian Ministry of Education, Universities and Research, PRIN 2010-11 (“Innovative methods for water resources management under hydro-climatic uncertainty scenarios”).

References

[1] W. Daily, A. Ramirez, D. J. La Brecque, J. Nitao, Electrical resistivity tomography of vadose zone water movement, Water Resour. Res. 28 (1992) 1429–1442.

[2] T. C. J. Yeh, J. Šimůnek, Stochastic fusion of information for characterizing and monitoring the vadose zone, Vadose Zone J. 1 (2002) 207–221.

[3] Q. Y. Zhou, J. Shimada, A. Sato, Temporal variations of the three-dimensional rainfall infiltration process in heterogeneous soil, Water Resour. Res. 38 (2002) 1–1–1–15.

[4] A. Binley, A. Kemma, Dc resisitivity and induced polarization methods, in: Y. Rubin, S. S. Hubbard (Eds.), Hydrogeophysics, volume 50, Springer, 2005, pp. 129–156.

[5] G. Cassiani, N. Ursino, R. Deiana, G. Vignoli, J. Boaga, M. Rossi, M. T. Perri, M. Blaschek, R. Duttmann, S. Meyer, R. Ludwig, A. Soddu, P. Dietrich, U. Werban, Non-invasive monitoring of soil static characteristics and dynamic states: a case study highlighting vegetation effects, Vadose Zone J. 11 (2012) vzj2011.0195.

[6] G. E. Archie, The electrical resistivity log as an aid in determining some reservoir characteristics, Trans. Am. Inst. Min. Metall. Eng. 146 (1942) 54–61.

[7] T. Ha, S. Pyun, C. Shin, Efficient electric resistivity inversion using adjoint state of mixed finite-element method for Poissons equation, J. Comp. Phys. 214 (2006) 171–186.

[8] E. Chung, T. Chan, X. Tai, Electrical impedance tomography using level set representations and total variation regularizationa, J. Comp. Phys. 205 (2005) 357–372.

[9] K. van den Doel, U. M. Ascher, On level set regularization for highly ill-posed distributed parameter estimation problems, J. Comp. Phys. 216 (2006) 707–723.

[10] W. Menke, Geophysical Data Analysis: Discrete Inverse Theory, Elsevier, New York, 1984.

[11] J. Rings, C. Hauck, Reliability of resistivity quantification for shallow subsurface water processes, J. Appl. Geophys. 68 (2009) 404–416.

[12] D. J. La Brecque, G. Heath, R. Sharpe, R. Versteeg, Autonomous

monitoring of fluid movement using 3-d electrical resistivity tomography, J. Environ. Eng. Geoph. 9 (2004) 167–176.

[13] A. M. Tartakovsky, D. Bolster, D. M. Tartakovsky, Hydrogeophysical approach for identification of layered structures of the vadose zone from electrical resistivity data, Vadose Zone J. 7 (2008) 1–8.

[14] K. Singha, S. M. Gorelick, Saline tracer visualized with three-dimensional electrical resistivity tomography: Field-scale spatial moment analysis, Water Resour. Res. 41 (2005) W05023.

[15] D. Michot, Y. Benderitter, A. Dorigny, B. Nicoullaud, D. King, A. Tabbagh, Spatial and temporal monitoring of soil water content with an irrigated corn crop cover using surface electrical resistivity tomography, Water Resour. Res. 39 (2003) 1138.

[16] J. Travelletti, P. Sailhac, J. P. Malet, G. Grandjean, J. Ponton, Hydrological response of weathered clay-shale slopes: water infiltration monitoring with time-lapse electrical resistivity tomography, Hydrol. Process. 26 (2012) 2106–2119.

[17] A. C. Hinnell, T. P. A. Ferré, J. A. Vrugt, J. A. Huisman, S. Moysey, J. Rings, M. Kowalsky, Improved extraction of hydrologic information from geophysical data through coupled hydrogeophysical inversion, Water Resour. Res. 46 (2010) W00D40.

[18] G. A. Hansen, C. Penland, On stochastic parameter estimation using data assimilation, Physica D 230 (2007) 88–98.

[19] P. J. Smith, S. L. Dance, M. J. Baines, N. K. Nichols, T. R. Scott, Variational data assimilation for parameter estimation: application to a simple morphodynamic model, Ocean Dyn. 56 (2009) 697–708.

[20] M. Camporese, C. Paniconi, M. Putti, P. Salandin, Ensemble Kalman filter data assimilation for a process-based catchment scale model of surface and subsurface flow, Water Resour. Res. 45 (2009) W10421.

[21] G. Evensen, The ensemble Kalman filter: theoretical formulation and practical implementation, Ocean Dyn. 53 (2003) 343–367.

[22] A. H. Jazwinski, Stochastic Processes and Filtering Theory, Academic Press, New York, 1970.

[23] P. Gauthier, P. Courtier R, P. Moll, Assimilation of simulated wind lidar data with a Kalman filter, Mon. Weather Rev. 121 (1993) 1803–1820.

[24] M. S. Arulampalam, B. Ristic, Comparison of the particle filter with range-parametrized and modified polar EKFs for angle-only tracking, in: Proc. SPIE, volume 4048, pp. 288–299.

[25] D. Pasetto, M. Camporese, M. Putti, Ensemble Kalman filter versus particle filter for a physically-based coupled surface-subsurface model, Adv. Water Resources 47 (2012) 1–13.

[26] N. J. Gordon, D. J. Salmond, A. F. M. Smith, Novel approach to nonlinear/non-Gaussian Bayesian state estimation, IEE Proc.-F 140 (1993) 107–113.

[27] A. Doucet, S. Godsill, C. Andrieu, On sequential Monte Carlo sampling methods for Bayesian filtering, Stat. Comput. 10 (2000) 197–208.

[28] H. Moradkhani, K.-L. Hsu, H. Gupta, S. Sorooshian, Uncertainty assessment of hydrologic model states and parameters: Sequential data assimilation using the particle filter, Water Resour. Res. 41 (2005) W05012.

[29] A. H. Weerts, G. Y. H. El Serafy, Particle filtering and ensemble Kalman filtering for state updating with hydrological conceptual rainfall-runoff models, Water Resour. Res. 42 (2006) W09403.

[30] Y. Zhou, D. McLaughlin, D. Entekhabi, Assessing the performance of the ensemble Kalman filter for land surface data assimilation, Mon. Weather Rev. 134 (2006) 2128–2142.

[31] K. L. Hsu, H. Moradkhani, S. Sorooshian, A sequential Bayesian approach for hydrologic model selection and prediction, Water Resour. Res. 45 (2009) W00B12.

[32] J. A. Vrugt, C. G. H. Diks, H. V. Gupta, W. Bouten, J. M. Verstraten, Improved treatment of uncertainty in hydrologic modeling: Combining the strengths of global optimization and data assimilation, Water Resour. Res. 41 (2005) W01017.

[33] H.-J. Hendricks Franssen, W. Kinzelbach, Real-time groundwater flow modeling with the ensemble Kalman filter: Joint estimation of states and parameters and the filter inbreeding problem, Water Resour. Res. 44 (2008) W09408.

[34] P. Salamon, L. Feyen, Assessing parameter, precipitation, and predictive uncertainty in a distributed hydrological model using sequential data assimilation with the particle filter, J. Hydrol. 376 (2009) 428–442.

[35] M. Camporese, C. Paniconi, M. Putti, P. Salandin, Comparison of data assimilation techniques for a coupled model of surface and subsurface flow, Vadose Zone J. 8 (2009) 837–845.

[36] D. A. Plaza, R. De Keyser, G. J. M. De Lannoy, L. Giustarini, P. Matgen, V. R. N. Pauwels, The importance of parameter resampling for soil moisture data assimilation into hydrologic models using the particle filter, Hydrol. Earth Syst. Sci. 16 (2012) 375–390.

[37] C. Montzka, H. Moradkhani, L. Weihermüller, H.-J. Hendricks Franssen, M. Canty, H. Vereecken, Hydraulic parameter estimation by remotely-sensed top soil moisture observations with the particle filter, J. Hydrol. 399 (2011) 410–421.

[38] J. Rings, J. A. Huisman, H. Vereecken, Coupled hydrogeophysical parameter estimation using a sequential Bayesian approach, Hydrol. Earth Syst. Sci. 14 (2010) 545–556.

[39] H. Haario, E. Saksman, J. Tamminen, An adaptive Metropolis algorithm, Bernoulli 7 (2001) 223–242.

[40] J. A. Vrugt, C. J. F. ter Braak, C. G. H. Diks, D. Higdon, B. A. Robinson, J. M. Hyman, Accelerating Markov chain Monte Carlo simulation by differential evolution with self-adaptive randomized subspace sampling, Int. J. Nonlinear Sci. Numer. Simul. 10 (2009) 273–290.

[41] J. S. Liu, R. Chen, Sequential Monte Carlo methods for dynamical systems, J. Am. Stat. Assoc. 93 (1998) 1032–1044.

[42] G. Kitagawa, Monte Carlo filter and smoother for non-Gaussian non-linear state space models, J. Comput. Graph. Stat. 5 (1996) 1–25.

[43] H. Moradkhani, C. M. DeChant, S. Sorooshian, Evolution of ensemble data assimilation for uncertainty quantification using the particle filter-Markov chain Monte Carlo method, Water Resour. Res. 48 (2012) W12520.

[44] J. A. Vrugt, C. J. F. ter Braak, C. G. H. Diks, G. Schoups, Hydrologic data assimilation using particle markov chain Monte Carlo simulation: Theory, concepts and applications, Adv. Water Resources 51 (2012) 457–478.

[45] M. Dowd, Bayesian statistical data assimilation for ecosystem models using Markov Chain Monte Carlo, J. Marine Syst. 68 (2007) 439–456.

[46] M. T. van Genuchten, D. R. Nielsen, On describing and predicting the hydraulic properties of unsaturated soils, Ann. Geophys. 3 (1985) 615–628.

[47] M. Camporese, C. Paniconi, M. Putti, S. Orlandini, Surface-subsurface flow modeling with path-based runoff routing, boundary condition-based coupling, and assimilation of multisource observation data, Water Resour. Res. 46 (2010) W02512.

[48] C. Paniconi, M. Putti, A comparison of Picard and Newton iteration

in the numerical-solution of multidimensional variably saturated flow problems, Water Resour. Res. 30 (1994) 3357–3374.

[49] A. Brovelli, G. Cassiani, E. Dalla, F. Bergamini, D. Pitea, A. M. Binley, Electrical properties of partially saturated sandstones: a novel computational approach with hydro-geophysical applications, Water Resour. Res. 41 (2005) W08411.

[50] A. Brovelli, G. Cassiani, Combined estimation of effective electrical conductivity and permittivity for soil monitoring, Water Resour. Res. 47 (2011) W08510.

[51] V. Nenna, A. Pidlisecky, R. Knight, Application of an extended Kalman filter approach to inversion of time-lapse electrical resistivity imaging data for monitoring recharge, Water Resour. Res. 47 (2011) W10525.

[52] G. Cassiani, A. Kemna, A. Villa, E. Zimmermann, Spectral induced polarization for the characterization of free-phase hydrocarbon contamination of sediments with low clay content, Near Surf. Geophys. 7 (2009) 547562.

[53] D. Canone, S. Ferraris, G. Sander, R. Haverkamp, Interpretation of water retention field measurements in relation to hysteresis phenomena, Water Resour. Res. 44 (2008) W00D12.

[54] M. Rossi, G. Manoli, D. Pasetto, R. Deiana, S. Ferraris, M. Putti, G. Cassiani, Quantitative hydro-gephysical monitoring and coupled modeling of a controlled infiltration experiment, Submitted (2013).

[55] G. Cassiani, M. Giustianini, S. Ferraris, R. Deiana, C. Strobbia, Time-lapse surface-to-surface gpr measurements to monitor a controlled infiltration experiment, Bollettino di Geofisica Teorica ed Apllicata 50 (2009) 209–226.

[56] M. Baudena, I. Bevilacqua, D. Canone, S. Ferraris, M. Previati, A. Provenzale, Soil water dynamics at a midlatitude test site: Field measurements and box modeling approaches, J. Hydrol. 414-415 (2012) 329–340.

[57] R. J. Hoeksema, P. K. Kitanidis, Analysis of the spatial structure of properties of selected aquifers, Water Resour. Res. 21 (1985) 563–572.

[58] G. Dagan, Flow and Transport in Porous Formations, Springer, New York, 1989.